Theor Appl Genet (2016) 129:717–728
DOI 10.1007/s00122-015-2660-4

ORIGINAL ARTICLE

The *yellow-fruited tomato 1* (*yft1*) mutant has altered fruit carotenoid accumulation and reduced ethylene production as a result of a genetic lesion in *ETHYLENE INSENSITIVE2*

Lei Gao[1,2] · Weihua Zhao[1,2] · Haiou Qu[1,2] · Qishan Wang[3] · Lingxia Zhao[1,2,4]

Received: 11 September 2015 / Accepted: 14 December 2015 / Published online: 8 January 2016

Abstract

Key message **The isolated *yft1* allele controls the formation of fruit color in *n3122* via the regulation of response to ethylene, carotenoid accumulation and chromoplast development.**

Abstract Fruit color is one of the most important quality traits of tomato (*Solanum lycopersicum*) and is closely associated with both nutritional and market value. In this study, we characterized a tomato fruit color mutant *n3122*, named as *yellow-fruited tomato 1* (*yft1*), which produces yellow colored mature fruit. Fruit color segregation of the progeny from an intra-specific cross (M82 × *n3122*) and an inter-specific cross (*n3122* × LA1585) revealed that a single recessive nuclear gene determined the yellow fruit phenotype. Through map-based cloning, the *yft1* locus was assigned to an 88.2 kb region at the top of chromosome 9 that was annotated as containing 12 genes. Sequencing revealed that one gene, *Solyc09g007870*, which encodes *ETHYLENE INSENSITIVE2* (*EIN2*), contained two mutations in *yft1*: a 13 bp deletion and a 573 bp insertion at position −318 bp upstream of the translation initiation site. We detected that *EIN2* expression was substantially lower in *yft1* than in the red-fruited M82 wild type and that, in addition, carotenoid accumulation was decreased, ethylene synthesis and perception were impaired and chromoplast development was delayed. The results implied that the reduced expression of *EIN2* in *yft1* leads to suppressed ethylene signaling which results in abnormal carotenoid production.

Introduction

Tomato (*Solanum lycopersicum*) is the second most highly produced vegetable crop worldwide after potato (*S. tuberosum*), with a production of 164 million tons, valued at ~$60 billion, in 2013 (http://faostat.fao.org/). Tomato fruit are

Communicated by S. Huang.

Electronic supplementary material The online version of this article (doi:10.1007/s00122-015-2660-4) contains supplementary material, which is available to authorized users.

✉ Lingxia Zhao
lxzhao@sjtu.edu.cn

Lei Gao
gaolei11@sjtu.edu.cn

Weihua Zhao
whzhao2013@163.com

Haiou Qu
quhaiou@163.com

Qishan Wang
wangqishan@sjtu.edu.cn

[1] Joint Tomato Research Institute, School of Agriculture and Biology, Shanghai Jiao Tong University, Shanghai 200240, China

[2] Plant Biotechnology Research Center, School of Agriculture and Biology, Shanghai Jiao Tong University, Shanghai 200240, China

[3] School of Agriculture and Biology, Shanghai Jiao Tong University, Shanghai 200240, China

[4] Key Laboratory of Urban Agriculture (South) Ministry of Agriculture, School of Agriculture and Biology, Shanghai Jiao Tong University, Shanghai 200240, China

used for both fresh consumption and in processing and they have been shown to have many beneficial effects on human nutrition and health (Adalid et al. 2010; Lin et al. 2014; Tanksley 2004). In addition, tomato is also a widely adopted experimental model plant in a wide range of plant research fields, including genetics (Chetelat et al. 2000; Tanksley 2004), evolution (Moyle 2008; Spooner et al. 2005), reproductive biology (Bedinger et al. 2011; Li and Chetelat 2010), genomics (Lin et al. 2014; Tomato Genome Consortium 2012), transcriptomics (Matas et al. 2011), proteomics (Yeats et al. 2010) and metabolomics (Alba et al. 2005; Osorio et al. 2011).

Tomato fruit quality is a major target for tomato breeders and consumers (Giovannoni 2006) and, in this regard, one aspect of particular interest is the color of the ripe fruit, which results from the accumulation of pigments such as carotenoid and flavonoids, as well as from chlorophyll degradation (Delgado-Vargas et al. 2000; Rosati et al. 2010). These pigments reduce damage from photo-oxidation and contribute to flower and fruit coloration which attracts insects and animals, thereby promoting pollination and seed dispersal. The pigments are also considered to be bioactive compounds and have been implicated in the prevention of cancer and cardiocerebrovascular disease in humans (Neto 2007; Riccioni 2009; Seeram et al. 2004; Wang et al. 2014).

Studies over the last decade, many involving mutants and transgenic lines, have helped elucidate the structural and regulatory pathways that influence mature fruit color. The fruit of some tomato genotypes appear pink, due to the reduced accumulation of the yellow flavonoid pigment naringenin chalcone in their peels. This was demonstrated by suppressing the expression of the key gene in flavonoid biosynthesis *CHS* (*CHALCONE SYNTHASE*), and in studies where *CHI* (*CHALCONE ISOMERASE*) was overexpressed, thereby reducing naringenin chalcone accumulation (Muir et al. 2001; Schijlen et al. 2007). Furthermore, a transcription factor MYB12 which regulated *CHS* expression has been shown to be the causal gene for the tomato colorless-peel *y* mutant, which has pink fruit (Adato et al. 2009; Ballester et al. 2010; Lin et al. 2014). The anthocyanin class of pigments is not typically detectable in cultivated tomato fruits, although the fruit of some wild tomato relatives have purple anthocyanin containing peels. Several genes associated with anthocyanin biosynthesis, including *AFT* (*ANTHOCYANIN FRUIT* from *S. chilense*), *ATV* (*ATROVIOLACEA* from *S. cheesmaniae*) and *ABG* (*AUBERGINE* from *S. lycopersicoides*), have been transferred into cultivated tomato, thereby creating purple fruited tomato lines with high anthocyanin levels (Gonzali et al. 2009). Moreover, the overexpression of *SlANT1*, a MYB transcription factor, resulted in purple spotting on the epidermis and pericarp of tomato fruits (Mathews et al. 2003).

Ripe fruits of the tomato mutant *gf* (*green-flesh*) remain green due to inhibited degradation of their thylakoid membranes, which hinders the developmental transition of chloroplasts into chromoplasts (Barry et al. 2008; Cheung et al.1993). In addition, the *SGR* (*STAY-GREEN*) gene is thought to be responsible for this mutated phenotype (Hörtensteiner 2009).

In addition to flavonoids and chlorophyll, carotenoid pigments are also important determinants of tomato fruit color, and each step in the carotenoid biosynthesis pathway has been studied in detail (Klee and Giovannoni 2011). Carotenoids comprise a class of isoprenoids, consisting of a 40 carbon long chain with a conjugated double bond. They are synthesized in the plastids from two geranylgeranyl diphosphates (GGPP), which are condensed into phytoene by phytoene synthase (PSY). Phytoene is then converted into all-*trans*-lycopene via the intermediate ζ-carotene product by phytoene desaturase (PDS), ζ-carotene isomerase (ZISO), ζ-carotene desaturase (ZDS) and *cis–trans* isomerase (CRTISO). Lycopene is located at the key branching point of α- and β-carotene, and is responsible for the red color of tomato fruits. The linear all-*trans*-lycopene can be converted into α-carotene, β-carotene and other xanthophylls through cyclization reactions and oxygenations by lycopene cyclase (LCY) and carotenoid hydroxylase (CHY) enzymes in the α-/β-carotene branches, respectively (Gao et al. 2015; Tomato Genome Consortium 2012).

PSY1 has been shown to be the rate-limiting enzyme in the carotenoid synthesis pathway and much research in tomato has focused on this enzyme and the corresponding gene. For example, *PSY1* has altered expression in the tomato mutants, *r* (*yellow-flesh*) and r^y, resulting in pale yellow fruit flesh and yellow fruit skin, respectively (Fray and Grierson 1993). Two mutational events, in an intron and in the 3′ untranslated region (UTR), of tomato *PSY1* (accession PI114490) led to a yellow-fruited phenotype, although the causal mechanism is still unknown (Yuan et al. 2008; Kang et al. 2014). Additionally, the mutated locus, r^{2997}, in a yellow-fleshed tomato was confirmed to be linked to *PSY1*, the transcripts of which were not detected (Kachanovsky et al. 2012). Isaacson et al. (2002) found that two orange-fruited tomato mutants, $tangerine^{mic}$ and $tangerine^{3183}$, accumulated pro-lycopene instead of all-trans-lycopene, and the two mutated loci were mapped to *CRTISO* (*CAROTENOID ISOMERASE*). Another example of a mutation in the carotenoid biosynthesis pathway is the orange-fruited mutant *Delta*, which accumulates δ-carotene at the expense of lycopene, and whose locus was shown by Ronen et al. (1999) to co-segregate with *LCY-E* (*LYCOPENE ε-CYCLASE*). Finally, the orange-fruited *Beta* and dark red-fruited *old-gold* mutants show increased β-carotene and lycopene levels, respectively, and the mutated loci were both mapped to *CYC-B*

Fig. 1 Fruit color of the parental lines and their progeny. **a** M82; **b** *n3122*; **c** LA1585; **d** F_1 progeny of *n3122* × LA1585; **e** the *red*-fruited F_2 progeny of *n3122* × LA1585; **f** the *yellow*-fruited F_2 progeny of *n3122* × LA1585; **g** F_1 progeny of M82 × *n3122*; **h** the *red*-fruited F_2 progeny of M82 × *n3122*; **i** the *yellow*-fruited F_2 progeny of M82 × *n3122*

(*CHROMOPLAST-SPECIFIC LYCOPENE β-CYCLASE*) (Ronen et al. 2000).

In addition to genes involved in carotenoid and flavonoids synthesis as well as chlorophylls degradation, several other genes have been shown to influence tomato fruit color formation. For example, the *high pigment* mutants (*hp-1*, *hp-2, hp-3*) exhibit higher fruit pigmentation due to elevated lycopene, flavonoid and chlorophyll levels, and have been mapped to *DDB1* (*UV-DAMAGED DNA BINDING PROTEIN 1*) (Lieberman et al. 2004), *DET1* (*DEETIOLATED1*) (Levin et al. 2003; Mustilli et al. 1999) and *ZEP* (*ZEAXANTHIN EPOXIDASE*) (Galpaz et al. 2008), respectively. Other regulators of fruit coloration include transcription factors associated with fruit ripening such as *RIN* (*RIPENING INHIBITOR*) (Vrebalov et al. 2002), *CNR* (*COLORLESS NON-RIPENING*) (Manning et al. 2006), *NOR* (*NON-RIPENING*) (Zhu et al. 2014) and components of the ethylene signaling transduction such as *NR* (*NEVER RIPE*) (Lanahan et al. 1994) and *EIN2* (*ETHYLENE INSENSITIVE2*) (Hu et al. 2010; Zhu et al. 2006).

Although it is well established that carotenoid, flavonoids and chlorophyll are involved in fruit coloration, the complex molecular mechanisms and regulatory networks governing their accumulation are still not well understood. In this study, we described the characterization of a yellow-fruited tomato mutant *n3122*, named as *yellow-fruited tomato 1* (*yft1*), including mapping of the underlying mutation, biochemical analysis of the carotenoid profiles and an evaluation of molecular processes associated with the phenotype, to better understand the determinants of fruit color.

Materials and methods

Plant material

Seeds of *n3122*, M82 (*S. lycopersicum*) and LA1585 (*S. pimpinellifolium*) (Fig. 1) were kindly provided by Prof. Dani Zamir (http://zamir.sgn.cornell.edu/mutateds) and the Tomato Genetics Resource Center (University of California, Davis, CA, USA, http://tgrc.ucdavis.edu), respectively. All the materials including M82, *n3122*, LA1585 and the mapping population were planted and grown under standard greenhouse conditions at the Pujiang experimental base, Shanghai Jiao Tong University, Shanghai, China.

Identification of the candidate gene

The two crosses, M82 × *n3122* and *n3122* × LA1585, were created for genetic analysis and the color of fully ripe fruit from each plant of the F_1 and F_2 generations was evaluated. The *n3122* × LA1585 F_2 population was also used to identify the candidate gene by map-based cloning. Eighty-nine plants, including 25 yellow-fruited and 64 red-fruited plants, were genotyped using 48 markers, which collectively covered the entire tomato genome, to create linkage groups with the mutated loci. These markers were chosen from the Sol Genomics Network (http://solgenomics.net/) or designed according to the sequence of the tomato genome (Table S1). A total of 1900 plants from the F_2 population were used to fine map the candidate gene using newly designed CAPS (cleaved amplified

polymorphic sequences) or dCAPS (derived cleaved amplified polymorphic sequences) markers (Table S1). Data were analyzed using R/qtl software (Broman et al. 2003).

Genes located in the mapped target region were identified using the tomato genome annotation (http://solgenomics.net/), and the candidate gene, *EIN2*, was amplified using LA Taq DNA polymerase (Takara, China) with the gene-specific primers 5′-ATGGAGTCTGAAACTCT GACTAGAG-3′ (forward) and 5′-TTACAAGACGAAAG GGGGTGATG-3′ (reverse) for the gene sequence from the start codon ATG to the stop codon TAA, 5′-GATGTT ATCGGGGAGGAAGA-3′ (forward) and 5′-TATTTGAT TTAAATGGTTAG-3′ (reverse) for the promoter sequence before the start codon ATG, and 5′-CTTGTTCATGTCA AATGGGTTG-3′ (forward) and 5′-AACCACAGCATCA GACAAAGAC-3′ (revere) for the nucleotide sequence around the start codon ATG.

EIN2 transcript levels were evaluated using quantitative real-time PCR (qRT-PCR). Total RNA was extracted using an RNAprep pure Plant Kit (Tiangen, China) from fruit pericarps of both M82 and *n3122* at 35 days post-anthesis (DPA), 47 DPA, 50 DPA and 54 DPA which corresponded to the MG (mature green), BR (breaker), BR + 3 (3 days after breaker) and RR (red ripe) stages of M82 as well as *n3122* at 60 DPA which corresponded to the BR stage in this genotype (Fig. S1). One μg total RNA was used as a template to synthesize cDNA using the PrimeScript™ RT Master Mix kit (Takara, China). qRT-PCR was performed in a 20 μL reaction volume containing 2 ng of cDNA and the SYBR premix *Ex-Taq* (Takara, China) with a qRT-PCR machine (Bio-Rad, UK). The PCR amplification program was 37 °C for 2 min and 94 °C 3 min, followed by 40 cycles of 94 °C for 20 s, 60 °C for 20 s and 72 °C for 20 s. Transcript levels were calculated using the $2^{-\Delta CT}$ equation (Kilambi et al. 2013), and *ACTIN* (Genbank Accession number BT013524) was used as a reference gene for gene expression normalization. *EIN2* gene-specific primers were 5′-ATGACAGGGATGATGGAGATTCG-3′ (forward) and 5′-TATGACCCCGGACCATCAGA-3′ (reverse) and *ACTIN* gene-specific primers were 5′- TTGCTGACCG-TATGAGCAAG-3′ (forward) and 5′-GGACAATGGATG-GACCAGAC-3′ (reverse).

Carotenoid measurements

Tomato fruit were collected from both M82 and *n3122* at 35 DPA, 47 DPA, 50 DPA and 54 DPA as well as *n3122* at 60 DPA. The equatorial region of the pericarp of the collected fruits was sampled in three biological replicates and ground to a fine powder in liquid nitrogen prior to high-performance liquid chromatography (HPLC) analysis. Extraction and quantification of carotenoid were carried out as previously described (Fraser et al. 2000) with some modifications. 500 mg fine powder sample was used for carotenoid extraction. The dried extracted residues were dissolved in 1 mL hexane and then filtered by a 0.22-μm filter. For carotenoid separation and detection, 60 μL of filtered solution was injected into a Hitachi L-2000 (Tokyo, Japan) HPLC system coupled with a reverse-phase C30 column (5 μm, 250 × 4.6 mm, YMC Inc., USA) and a diode-array detector monitoring continuously from 220 to 500 nm. The elution programme using methanol (A), water/methanol (v:v = 20:80) with 0.2 % ammonium acetate (B) and tert-methyl butyl ether (C) as the mobile phases with 1 ml·min-1 flow rate was carried out as follows: initially an isocratic step of 95 % A, 5 % B for 12 min; then three linear gradient steps: firstly, the mobile phases changed to 80 % A, 5 % B, 15 % C by 5 min, secondly to 50 % A, 5 % B, 45 % C by 10 min, thirdly to 25 % A, 5 % B, 70 % C by 10 min; subsequently isocratically for 13 min. One more linear gradient step of 5 min was performed to return to the initial concentrations of the mobile phase, then maintaining 15 min for equilibrating the column. Carotenoid identification was conducted by the comparison of characteristic absorption spectra and retention time with authentic standards. Carotenoid quantification was calculated using a dose–response curve created by standards. Lycopene, β-carotene, zeaxanthin and lutein standards were purchased from the Sigma Chemical Co. (Sigma, USA) and α-carotene from Santa Cruz Biotechnology, Inc. (Santa Cruz, USA).

Chromoplast ultrastructure visualization

The ultrastructure of plastids in the pericarp of 35 DPA, 47 DPA, 50 DPA and 54 DPA fruit of both the M82 and *n3122* genotypes was examined, as well as those from 60 DPA *n3122* fruit, using transmission electron microscopy (TEM), as previously described (Schweiggert et al. 2011) with some modifications. Small pieces (1–2 mm^2) were cut from the mesocarp and immediately immersed into 2.5 % glutaraldehyde in 0.1 M phosphate buffer (17.55 g $Na_2HPO_4{\cdot}12H_2O$ and 7.95 g $NaH_2PO_4{\cdot}2H_2O$ per L, pH 6.8) for 5 h at 4 °C and a vacuum was applied for 30 min to ensure efficient fixation. The samples were washed three times for 20 min in a 0.1 M phosphate buffer. A post-fixation step with 2 % osmium tetroxide in 0.1 M phosphate buffer for 3 h followed by three washes in the 0.1 M phosphate buffer. Subsequently, after dehydration with 50 % ethanol for 20 min, the samples were stained with 2 % uranyl acetate in 70 % ethanol for 12 h. Sequential dehydration in a series of ethanol and acetone grades as 70 % ethanol, 90 % ethanol, 90 % ethanol and 90 % acetone (v:v = 1:1), 90 % acetone, 100 % acetone was then performed for 20 min per grade. The dehydrated samples were immersed in acetone and epoxy resin 812 (Hede Biotechnology Co.

Ltd., China) (v:v = 1:1 for 6 h, v:v = 1:2 for 12 h) and then twice in epoxy resin 812 for 24 h. After that, the samples were again immersed in epoxy resin 812 and kept at 65 °C for 48 h for polymerization. Finally, 70 nm thick sections were isolated from the samples using a Leica UC6-FC6 microtome with a diamond knife (Leica Microsystems Inc., Germany). These ultrathin sections were stained with lead citrate and imaged using TEM (Tecnai G2 Spirit Biotwin, USA).

Responses to ethylene

Tomato fruit were collected from both M82 and *n3122* at 35 DPA, 47 DPA, 50 DPA and 54 DPA, as well as at 60 DPA from *n3122*. The fruit were weighed and kept at 25 °C for 2 h prior to ethylene measurements to allow the harvesting-induced burst of ethylene synthesis to subside. To measure endogenous ethylene levels, fruits from each time point ($n = 5$) were sealed in 500 mL airtight bottles and kept at 25 °C for 4 h, before 1 mL headspace gas was taken from the bottle and injected into a gas chromatograph (GC-2010, Shimadzu Corporation, Japan) equipped with an HP-PLOT/Q column and a flame ionization detector. The injector temperature was set at 200 °C and the flame ionization detector at 250 °C. The oven temperature was initially set at 40 °C for 5 min and then increased to 220 °C at a rate of 30 °C/min. The endogenous ethylene concentration (nL g^{-1} h^{-1}) was calculated using a dose–response curve created with a 10 ppm ethylene standard.

The responses of tomato fruit and seedlings to exogenous ethylene were measured as follows. The MG stage fruit (35 DPA, $n = 3$) from M82 and *n3122* were separately sealed in 500 mL airtight bottles with 20 ppm ethylene. The fruit were held at 25 °C for 24 h, before the fruits were removed and then left at 25 °C to evaluate their ripening. Seeds from both M82 and *n3122* were sterilized with 75 % ethanol for 2 min and 25 % NaClO for 10 min, and then rinsed three times in sterile water. The sterilized seeds were germinated on Murashige and Skoog (MS) medium (Sigma, USA) with or without 10 μM 1-aminocyclopropane-1-carboxylic acid (ACC) (Sigma, USA) in petri dishes at 28 °C in the dark, and the lengths of the hypocotyls and the roots were measured on day 8 after sowing.

Results

Characterization of the *n3122* phenotype

The *n3122* mutant, which was identified from a fast-neutron irradiation treated M82 population (Menda et al. 2004), produced yellow fruit whose color was readily distinguishable from the red-fruited wild type M82 (Fig. 1). We determined that the *n3122* fruit showed delayed ripening and reached the BR stage at 60 DPA, in contrast to the M82 fruit which reached the BR stage at 47 DPA (Fig. S1).

A single recessive *yft1* allele is associated with the *n3122* yellow fruit phenotype

To investigate the genetic basis of the *n3122* yellow fruit phonotype, two crosses (*n3122* × LA1585 and M82 × *n3122*) were made and the fruit color of the progeny was evaluated. All fruits from both crosses appeared red (18 F_1 plants of *n3122* × LA1585 and 12 F_1 plants of M82 × *n3122*) in the F_1 generation, whereas both red and yellow fruit were produced by plants of the F_2 generation, with a segregation ratio of 79:25 and 58:13 (red:yellow) for *n3122* × LA1585 and *n3122* × M82, respectively (Table 1). And the Chi square (χ^2) values of red-fruited plants: yellow-fruited plants were 0.0128 for *n3122* × LA1585 ($\chi^2_{0.05} = 3.84$, $p > 0.05$) and 1.357 for *n3122* × M82, ($\chi^2_{0.05} = 3.84$, $p > 0.05$) (Table 1), which fits the theoretical Mendelian ratio of 3:1, suggesting that the phenotype is controlled by a single recessive allele, *yft1*.

Fine mapping and identification of a candidate gene underlying *yft1*

To identify the *yft1* candidate gene underlying the mutant phenotype, the F_2 generation (*n3122* × LA1585) was used as a mapping population. A total of 89 individuals (25 yellow- and 64 red-fruited) were used to construct linkage groups with 48 molecular markers that were evenly distributed among the 12 tomato chromosomes. *yft1* was initially mapped to a position between the CAPS markers 9-29 and cLEX-3-N24, which is a ~1 Mb region at the top of chromosome 9. Subsequently, 1900 F_2 plants were used for fine mapping, and the *yft1* gene was finally assigned to an 88.2 kb region between CAPS markers 9-S and 9-R (Fig. 2a). According to the tomato genome annotation (ITAG2.3, http://solgenomics.net), a total of 12 genes are located in this target region (Table 2); however, of these, only one, *Solyc09g007870*, which is annotated as encoding the ETHYLENE INSNSITIVE2 (EIN2) protein, has been shown to be essential for the ethylene signal transduction pathway and to be involved in regulating fruit ripening (Zhu et al. 2006; Hu et al. 2010). Nucleotide sequencing revealed that there were no differences in the DNA-coding sequences of the *EIN2* gene from *n3122* and wild type M82 (Fig. S2). However, a 13 bp deletion and a 573 bp insertion were found at -318 bp upstream of the translation initiation codon of *EIN2* in *n3122* (Fig. 2b, Fig. S3). Moreover, *EIN2* expression was significantly down-regulated in *n3122* at all tested time points between 35 DPA and 60 DPA (Fig. 2c), indicating that *EIN2* is a candidate gene for *yft1*.

Table 1 Segregation of fruit color in the segregating populations

Combination	Generation	Total plants	Red fruit plants	Yellow fruit plants	Expected ratio	χ^2 value
*n*3122 × LA1585	F_1	18	18			
	F_2(a)	104	79	25	3:1	0.0128
	F_2(b)	1900	1446	454	3:1	1.180
M82 × *n3122*	F_1	12	12			
	F_2	71	58	13	3:1	1.357

F_2(a) for primary mapping of the *yft1*; F_2(b) for fine mapping of the *yft1*

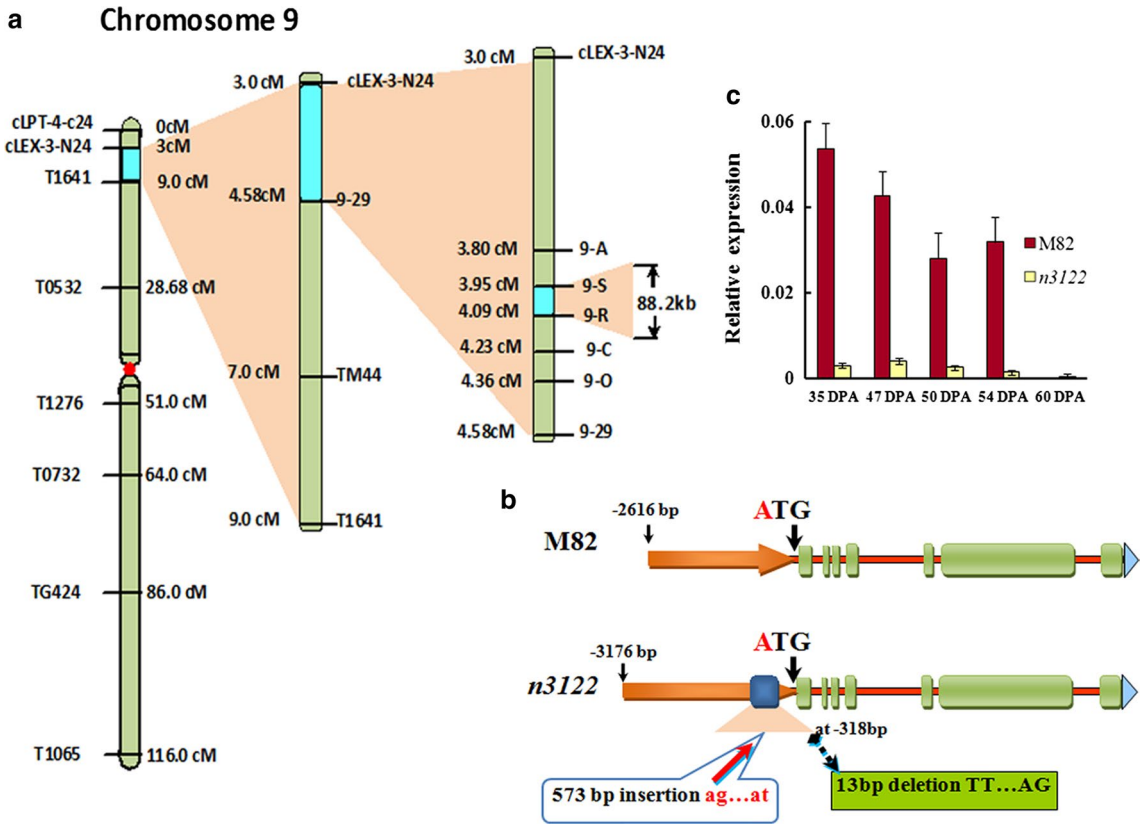

Fig. 2 *EIN2* is a candidate gene for the *n3122* mutation. **a** Schematic view of the map-based cloning; **b** mutation events, a 13 bp deletion and a 573 bp insertion at position −318 bp upstream of the translation initiation site (ATG) of *EIN2* in *n3122*; **c** transcriptional expression of *EIN2* in M82 and *n3122* fruits at different developmental stages

n3122 fruit show reduced carotenoid accumulation and delayed chromoplast development

The carotenoid profiles of fruit from both M82 and *n3122* were evaluated by HPLC to determine the cause of the yellow fruit color. Both the composition and content of carotenoid were significantly different between *n3122* and M82, such that M82 showed a substantial increase in total carotenoid levels during fruit development from 35 DPA (MG) to 54 DPA (BR + 7), with the highest concentration of 102.8 μg g^{-1} fresh weight (FW) at 54 DPA, which was an approximately 20-fold increase compared to 35 DPA (5.1 μg g^{-1} FW). In contrast, the total carotenoid levels were consistently low (6.3 μg g^{-1} FW avg.) in *n3122*, and the content was only 6 % of that of M82 fruit at 54 DPA (Fig. 3a).

Based on HPLC analysis, levels of the carotenoid lycopene, α-carotene, β-carotene and lutein, were significantly different between extracts form *n3122* and M82 fruit, while zeaxanthin was not detectable at any stage. Lycopene began to accumulate at 47 DPA and the levels increased sharply with fruit ripening, reaching a peak of 86 μg g^{-1} FW at 54 DPA, thereby contributing up to 83 % of the total carotenoid in M82. However, lycopene was completely absent

Table 2 Twelve predicted genes in the 88.2-kb mapping region at the chromosome 9 in tomato

Gene Locus	Annotation	Physical position
Solyc09g007830	Cytokinin riboside 5′-monophosphate phosphoribohydrolase	SL2.50ch09:1356808..1361135
Solyc09g007840	Cyclic nucleotide gated channel; Cyclic nucleotide binding	SL2.50ch09:1373797..1376961
Solyc09g007850	RNA-binding protein; RNA recognition motif, RNP-1	SL2.50ch09:1377722..1380930
Solyc09g007860	Plant synaptotagmin; C2 membrane targeting protein	SL2.50ch09:1382071..1388219
Solyc09g007870	Manganese transporter mntH; Ethylene-insensitive 2	SL2.50ch09:1401117..1407730
Solyc09g007880	Unknown protein	SL2.50ch09:1413116..1413295
Solyc09g007890	Phenylalanine ammonia-lyase	SL2.50ch09:1413536..1415858
Solyc09g007900	Phenylalanine ammonia-lyase	SL2.50ch09:1419041..1422226
Solyc09g007910	Phenylalanine ammonia-lyase	SL2.50ch09:1429132..1437334
Solyc09g007920	Phenylalanine ammonia-lyase	SL2.50ch09:1435451..1440492
Solyc09g007930	Unknown protein	SL2.50ch09:1438321..1439339
Solyc09g007940	Adenosine kinase	SL2.50ch09:1440058..1444221

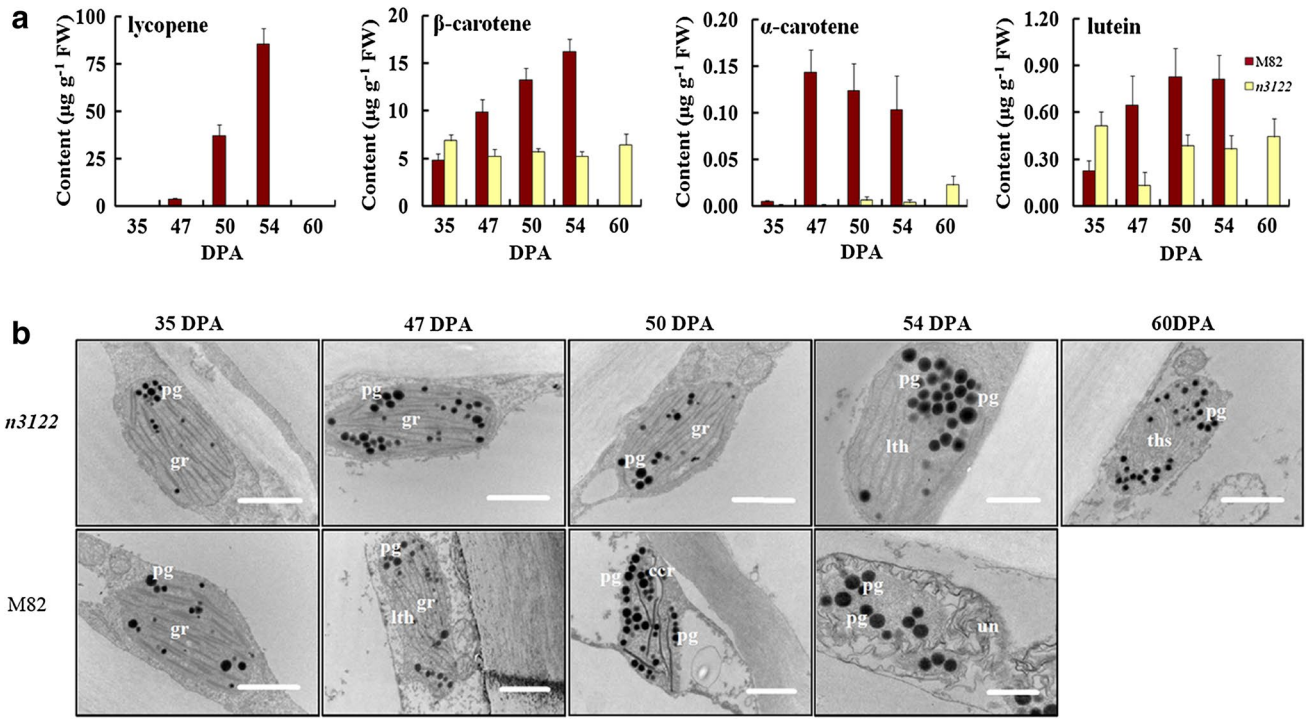

Fig. 3 Inhibition of carotenoid accumulation in *n3122*. **a** Carotenoid contents including lycopene, α-carotene, β-carotene and lutein, value = mean ± SD ($n = 3$). **b** Plastid ultrastructure in M82 and *n3122* fruit at different development stages. *pg* plastoglobule, *gr* grana, *lth* long linear thylakoid membrane structure, *ccr* carotenoid crystalloids, *um* undulating membrane representing the lost carotenoid crystalloids. *ths* thylakoid membrane with swollen compartment. *Bars* 500 nm

from all developmental stages of *n3122*. β-carotene accumulation gradually increased in M82 from 35 DPA to 54 DPA, where it reached a peak of 16.2 μg g^{-1} FW, equal to 16 % of the total carotenoid concentration. In contrast, β-carotene levels in *n3122* were relatively consistent (5.3–6.9 μg g^{-1} FW) and represented up to 90 % of the total carotenoid. The concentration of α-carotene decreased with fruit development in M82 from 47 DPA to 54 DPA, while lutein content increased, suggesting that lutein accumulated at the expense of α-carotene. The levels of both these compounds remained at relatively low levels in *n3122*.

We next examined the ultrastructure of the plastids using TEM, to explore carotenoid storage and chromoplast development in *n3122*. Typical lens-shaped chloroplasts were

observed at 35 DPA in both M82 and *n3122*. In the later BR stages of M82 fruit (47 DPA), the tightly stacked grana organization was rapidly disrupted and replaced by the linear thylakoid membrane structures with swollen compartments which also disappeared at 50 DPA. The number of plastoglobules gradually increased from 35 DPA to 50 DPA, and crystalloid structures and undulating membranous structures appeared at 50 to 54 DPA. In contrast, the lens-shaped chloroplasts were constantly observed in 35 DPA to 50 DPA *n3122* fruit and the grana organization was gradually disassembled during fruit development. Although the linear thylakoid membrane structures and even some swollen thylakoid compartments were observed in later stage, the crystalloids or undulating membranous structures were not observed all along (Fig. 3b). These observations indicated that chromoplast development was delayed in *n3122* fruit, coincident with the abnormal production of carotenoid accumulation.

n3122 shows impaired ethylene synthesis and perception

The *yft1* candidate gene, *EIN2,* is known to be a key component of ethylene signaling transduction (Qiao et al. 2012), and so we hypothesized that the reduced expression of *EIN2* in *n3122* might impair ethylene synthesis and perception. To test this, we measured ethylene production from both M82 and *n3122* fruit. Ethylene biosynthesis by fruit of both genotypes was relatively low at 35 DPA, but subsequently increased sharply in M82, reaching a peak of 7.33 nL g^{-1} h^{-1} FW at 47 DPA (approximately, 14-fold greater than at 35 DPA), before gradually decreasing to 4.95 nL g^{-1} h^{-1} FW at 54 DPA. In contrast, *n3122* fruit showed a slow increase in ethylene production from 35 DPA to 54 DPA (1.72 nL g^{-1} h^{-1} FW), and the amounts of ethylene produced by 47 DPA, 50 DPA, and 54 DPA fruit were significantly lower than those of M82 ($p < 0.001$). Although a rapid increase in ethylene levels occurred at 60 DPA, reaching 5.20 nL g^{-1} h^{-1} FW, they were still significantly lower than levels produced by M82 fruit at 47 DPA (BR stage, $p < 0.05$ level) (Fig. 4a).

To assess ethylene perception, MG fruits were exposed to exogenous ethylene (20 ppm) for 24 h. The M82 fruits reached the BR stage on day 7 after treatment, which was 5 days faster than normally developing fruit (i.e., no treatment). However, treated *n3122* fruit took 13 days to transition from MG to BR (Fig. 4d). To test the sensitivity of the *n3122* seedling to ethylene, an ethylene triple response assay (Lanahan et al. 1994) was conducted. The M82 and *n3122* seedlings showed no differences in hypocotyl and root length, when grown without exogenous ACC. However, in the presence of 10 μM ACC *n3122* hypocotyls and roots were significantly longer than those of M82 ($p < 0.001$) (Fig. 4b, c). Both roots and hypocotyls were significantly shorter under these conditions in both genotypes compared to those grown without ACC ($p < 0.001$). These results suggested that *n3122* exhibited partial insensitivity to ethylene.

Discussion

EIN2 is a candidate gene for the *n3122 yft1* mutation

The tomato mutant, *n3122*, produced characteristic yellow colored fruit and showed perturbed ripening. Using map-based cloning, the mutated locus was determined to be located within an 88.2 kb region that was predicted to contain 12 genes. Comparing the known functions of these genes to the phenotype of the *n3122* fruits, we focused on *Solyc09g007870*, which encodes EIN2. Two mutations were found in the promoter region of *EIN2*, and its transcript levels were significantly lower in *n3122* than in wild type M82.

The *EIN2* gene (*AtEIN2*) was first cloned from *Arabidopsis thaliana* by map-based cloning using a loss-of-function mutant that showed complete ethylene insensitivity. *AtEIN2* encodes a 1294 amino acid protein with 12 transmembrane helices in the N-terminus (residues 1–461) and a hydrophilic C-terminal domain (residues 462–1294) (Alonso et al. 1999). The residue 1262–1269 region corresponds to a nuclear localization signal (NLS), which is important for nuclear import of the C-terminal domain and the formation of the EIN2-ETR1 (ETHYLENE RESPONSE1) complex (Bisson and Groth 2011, 2015). *EIN2* is a key component of the ethylene signal transduction pathway as it links ethylene perception in the endoplasmic reticulum (ER) with the response in the nucleus (Wang and Wen 2015). It has been demonstrated that in *A. thaliana* EIN2 acts downstream of the ethylene receptors and the Raf-like protein kinase, CTR1 (CONSTITUTIVE TRIPLE RESPONSE1), and that it interacts with ETR1 and CTR1 in the ER to regulate ethylene signaling (Bisson et al. 2009). In the absence of ethylene, the receptors activate CTR1, which directly phosphorylates EIN2 to inhibit an ethylene response. In the presence of ethylene, the C terminus of un-phosphorylated EIN2 is cleaved and translocated to the nucleus to activate the ethylene response via the transcription factors, EIN3/EIL1 (ETHYLENE INSENSITIVE LIKE1) (Ju et al. 2012; Qiao et al. 2012; Wen et al. 2012).

In addition to *A. thaliana*, *EIN2* genes have been characterized from rice (*Oryza sativa*) (Jun et al. 2004), petunia (*Petunia hybrida*) (Shibuya et al. 2004), maize (*Zea mays*) (Gallie and Young 2004) and tomato (Wang et al. 2007). *SlEIN2* from tomato was isolated by Wang et al.

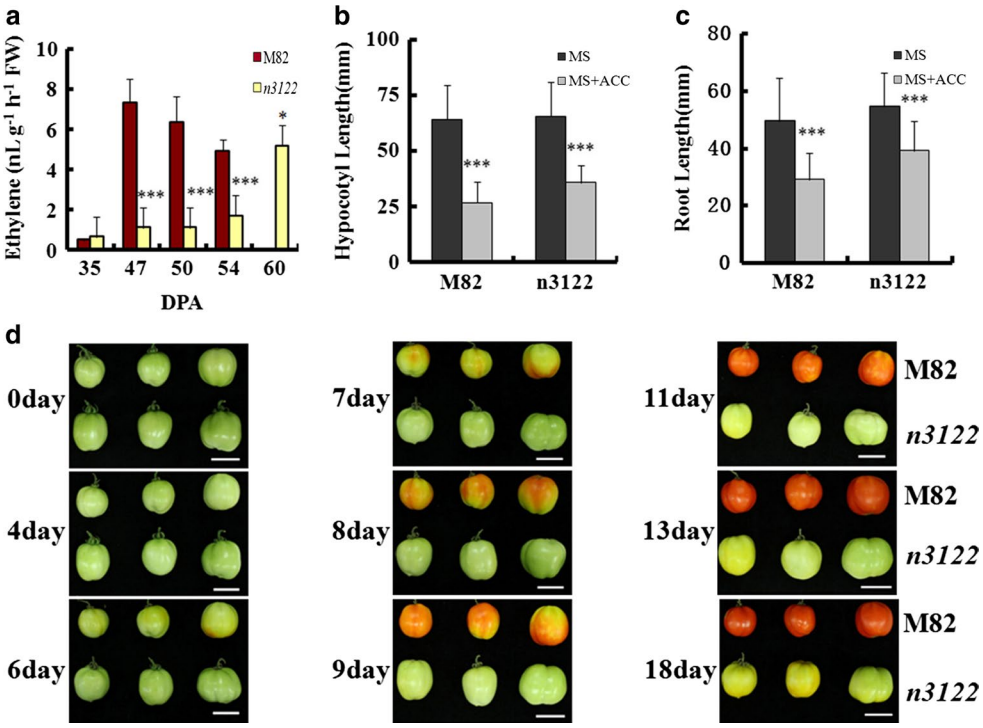

Fig. 4 Ethylene synthesis and perception is partially impaired in *n3122*. **a** Ethylene production by M82 and *n3122* fruit at different developmental stages. *Error bars* indicate SD ($n = 5$), *triple asterisks* and *single asterisk* indicate that ethylene release from *n3122* fruits was significantly lower than that from M82 at the $p < 0.001$ and $p < 0.05$ level, respectively (Student's *t* test). FW, fresh weight. **b** Hypocotyl length in 8-day old seedlings. *Error bars* indicate SD (n = 24), *triple asterisks* indicate a *P* value <0.001. **c** Root length of 8-day old seedlings. *Error bars* indicate SD ($n = 24$), ***$p < 0.001$. **d** changes in tomato fruit color on the day after MG stage fruit were exposed to exogenous ethylene (20 ppm) for 24 h, *bars* 3 cm

(2007) using the rapid amplification of cDNA ends method (RACE); however, we note that the published sequence from that study (Genbank No. XM_010327408), derived from the tomato cultivar Ailsa Craig, is different in several nucleotides from the sequence obtained in this present study. Zhu et al. (2006) used a TRV-based VIGS system to reduce *EIN2* expression in tomato fruits, resulting in *EIN2*-silenced fruit with distinct regions that were either green and non-ripening, or soft and red. In addition, Hu et al. (2010) constructed a *LeEIN2*-silenced transgenic tomato line that had hard yellow fruit at the BR + 4 stage and seedlings with partially impaired ethylene sensitivity. In this current study, impaired fruit ripening, as evidenced by a yellow fruit color, and insensitivity to ethylene were also observed in *n3122*. These phenotypes, taken together with the results from Zhu et al. (2006) and Hu et al. 2010), support the hypothesis that *EIN2* is the candidate gene responsible for the *n3122* phenotypes.

yft1 regulates fruit coloration via ethylene action

As a climacteric berry fruit, tomato requires ethylene to ripen (Klee and Giovannoni 2011). The ripening deficient mutant *Nr* has a mutation in the ethylene receptor, which functions upstream of EIN2 in the ethylene signaling transduction pathway, and also has ripening-impaired fruits with a yellow/orange color (Lanahan et al. 1994; Wilkinson et al. 1995). Down-regulation of the tomato ethylene synthesis-associated genes, *ACS4* (*1-AMINOCYCLOPROPANE-1-CARBOXYLIC ACID SYNTHETASE 4*), *ACS2* and *ACO1* (*1-AMINOCYCLOPROPANE-1-CARBOXYLIC ACID OXIDASE 1*), prevents fruit ripening (Hamilton et al.1990; Oeller et al. 1991; Picton et al. 1993), and the ripening-deficient mutants, *rin* (Vrebalov et al. 2002), *cnr* (Manning et al. 2006) and *nor* (Zhu et al. 2014), which all have hard yellow/orange mature fruits, have mutations in transcription factors that regulate fruit ripening at least partially via an ethylene dependent pathway (Karlova et al. 2014). Thus, blocking ethylene synthesis or perception in tomato results in ripening-deficient fruit with altered color. In this study, of the 12 genes located in the target region identified via map-based cloning, only *EIN2* was annotated as being related to ethylene perception or synthesis. Based on the results reported in this study, we conclude that the *yft1* is a new *EIN2* allelic mutant that produces yellow fruit as a consequence of reduced ethylene biosynthesis.

Tomato fruit color in large part reflects the composition and content of carotenoid (Fray and Grierson 1993), with the carotenoid pigment, lycopene, being responsible for the red color. In fully ripe fruit of most red-fruited tomato varieties, lycopene contributes 70–90 % of the total carotenoid, while the orange pigment β-carotene accounts for 5–40 % (Ma et al. 2014). In this study, lycopene and β-carotene represented 83 and 16 % of the total carotenoid levels in M82 fruit, respectively. However, lycopene was not detectable in *n3122* fruit and the total carotenoid levels were ~6 % of those in M82 fruit. The carotenoid profile of

M82 was reported by Ronen et al. (2000), and showed, in agreement with our results, that the lycopene accounted for 90 %, followed by β-carotene (5 %) and then lutein. Lycopene is completely absent from the yellow-fruited tomato mutant r^{2997} and the levels of total carotenoid, which were composed largely of β-carotene and lutein, were only ~4 % of those in the wild type fruit (Kachanovsky et al. (2012). Similarly, lycopene was also not detected in the yellow-fruited tomato line, PI114490 (Yuan et al. 2008), and we inferred that the yellow fruit color of *n3122* reflects a decrease in carotenoid accumulation, and especially of lycopene.

Plastids play a central role in the synthesis and storage of carotenoid. Harris and Spurr (1969a, b) observed two carotenoid crystalloid substructures in normally ripening red tomato and the *Beta* mutant but not in the yellow-fruited *r* mutant. One was a high electron-dense crystalloid, and the other was an undulating membrane representing the crystalloids which were lost during dehydration. Schweiggert et al. (2011) also found carotenoid crystalloids in red papaya (*Carica papaya*) but not in yellow papaya, which contained only trace amount of lycopene, and similar results were obtained in studies of red- and white-fleshed loquat (*Eriobotrya japonica*) fruits (Fu et al. 2012). In this current study, both the highly dense crystalloids and the transparent undulating membranes were observed in M82 but not in *n3122*. The carotenoid profiles were consistent with the changes in chromoplast ultrastructure in both *n3122* and wild type M82, and the chloroplast-to-chromoplast transition and carotenoid accumulation coincided with ethylene production in both M82 and *n3122*. This suggests that *yft1* regulates fruit coloration via ethylene action, but how ethylene influences this biological process has yet to be determined.

Author contribution statement LG and LXZ designed the research and wrote the manuscript; LG performed qRT-PCR, TME, HPLC and primary mapping; WHZ performed fine mapping; HOQ measured ethylene; WQS analyzed map-based cloning data.

Acknowledgments We would like to thank Dr. Dani Zamir and TGRC (UC, Davis) for providing tomato seeds. We appreciate help from the Instrumental Analysis Center of Shanghai Jiao Tong University with TEM work. We thank PlantScribe (www.plantscribe.com) for carefully editing this manuscript. This work was supported by Grants from the Key Technology Research and Development Program of Shanghai Science and Technology Committee (No. 14JC1403400), the National Natural Science Foundation of China (No. 31071810), the China National '863' High-Tech Program (No. 2011AA100607) and Shanghai Jiao Tong University Agri-X Fund (2015).

Compliance with ethical standards

Conflict of interest The authors declare no competing or financial interests.

Ethical standards All the experiments performed in this study comply with the current laws of China.

References

Adalid AM, Rosello S, Nuez F (2010) Evaluation and selection of tomato accessions (*Solanum* section *Lycopersicon*) for content of lycopene, β-carotene and ascorbic acid. J Food Compos Anal 23:613–618

Adato A, Mandel T, Mintz-Oron S, Venger I, Levy D, Yativ M, Domínguez E, Wang Z, De Vos RCH, Jetter R (2009) Fruit-surface flavonoid accumulation in tomato is controlled by a SlMYB12-regulated transcriptional network. PLoS Genet 5:e1000777

Alba R, Payton P, Fei Z, McQuinn R, Debbie P, Martin GB, Tanksley SD, Giovannoni JJ (2005) Transcriptome and selected metabolite analyses reveal multiple points of ethylene control during tomato fruit development. Plant Cell 17:2954–2965

Alonso JM, Hirayama T, Roman G, Nourizadeh S, Ecker JR (1999) EIN2, a bifunctional transducer of ethylene and stress responses in Arabidopsis. Science 284:2148–2152

Ballester AR, Molthoff J, de Vos R, Hekkert BTL, Orzaez D, Fernandez-Moreno JP, Tripodi P, Grandillo S, Martin C, Heldens J, Ykema M, Granell A, Bovy A (2010) Biochemical and molecular analysis of pink tomatoes: deregulated expression of the gene encoding transcription factor S1MYB12 leads to pink tomato fruit color. Plant Physiol 152:71–84

Barry CS, McQuinn RP, Chung M-Y, Besuden A, Giovannoni JJ (2008) Amino acid substitutions in homologs of the STAY-GREEN protein are responsible for the *green-flesh* and *chlorophyll retainer* mutations of tomato and pepper. Plant Physiol 147:179–187

Bedinger PA, Chetelat RT, McClure B, Moyle LC, Rose JK, Stack SM, van der Knaap E, Baek YS, Lopez-Casado G, Covey PA, Kumar A, Li W, Nunez R, Cruz-Garcia F, Royer S (2011) Interspecific reproductive barriers in the tomato clade: opportunities to decipher mechanisms of reproductive isolation. Sex Plant Reprod 24:171–187

Bisson MMA, Groth G (2011) New paradigm in ethylene signaling: EIN2, the central regulator of the signaling pathway, interacts directly with the upstream receptors. Plant Signal Behav 6:164–166

Bisson MMA, Groth G (2015) Targeting plant ethylene responses by controlling essential protein-protein interactions in the ethylene pathway. Mol Plant 8:1165–1174

Bisson MMA, Bleckmann A, Allekotte S, Groth G (2009) EIN2, the central regulator of ethylene signalling, is localized at the ER membrane where it interacts with the ethylene receptor ETR1. Biochem J 424:1–6

Broman KW, Wu H, Sen Ś, Churchill GA (2003) R/qtl: QTL mapping in experimental crosses. Bioinformatics 19:889–890

Chetelat RT, Meglic V, Cisneros P (2000) A genetic map of tomato based on BC_1 *Lycopersicon esculentum* × *Solanum lycopersicoides* reveals overall synteny but suppressed recombination between these homeologous genomes. Genetics 154:857–867

Cheung AY, McNellis T, Piekos B (1993) Maintenance of chloroplast components during chromoplast differentiation in the tomato mutant *green flesh*. Plant Physiol 101:1223–1229

Delgado-Vargas F, Jimenez AR, Paredes-Lopez O (2000) Natural pigments: carotenoid, anthocyanins, and betalains–characteristics, biosynthesis, processing, and stability. Crit Rev Food Sci Nutr 40:173–289

Fraser PD, Pinto MES, Holloway DE, Bramley PM (2000) Application of high-performance liquid chromatography with photodiode array detection to the metabolic profiling of plant isoprenoids. Plant J 24:551–558

Fray RG, Grierson D (1993) Identification and genetic analysis of normal and mutant phytoene synthase genes of tomato by sequencing, complementation and co-suppression. Plant Mol Biol 22:589–602

Fu X, Kong W, Peng G, Zhou J, Azam M, Xu C, Grierson D, Chen K (2012) Plastid structure and carotenogenic gene expression in red-and white-fleshed loquat (*Eriobotrya japonica*) fruits. J Exp Bot 63:341–354

Gallie D, Young T (2004) The ethylene biosynthetic and perception machinery is differentially expressed during endosperm and embryo development in maize. Mol Genet Genomics 271:267–281

Galpaz N, Wang Q, Menda N, Zamir D, Hirschberg J (2008) Abscisic acid deficiency in the tomato mutant *high-pigment 3* leading to increased plastid number and higher fruit lycopene content. Plant J 53:717–730

Gao M, Qu H, Gao L, Chen L, Sebastian RS, Zhao L (2015) Dissecting the mechanism of *Solanum lycopersicum* and *Solanum chilense* flower colour formation. Plant Biol 17:1–8

Giovannoni JJ (2006) Breeding new life into plant metabolism. Nat Biotechnol 24:418–419

Gonzali S, Mazzucato A, Perata P (2009) Purple as a tomato: towards high anthocyanin tomatoes. Trends Plant Sci 14:237–241

Hamilton A, Lycett G, Grierson D (1990) Antisense gene that inhibits synthesis of the hormone ethylene in transgenic plants. Nature 346:284–287

Harris WM, Spurr AR (1969a) Chromoplasts of tomato fruits. I. Ultrastructure of low-pigment and high-beta mutants. Carotene analyses. Am J Bot 56:369–379

Harris WM, Spurr AR (1969b) Chromoplasts of tomato fruits. II. The red tomato. Am J Bot 56:380–389

Hörtensteiner S (2009) Stay-green regulates chlorophyll and chlorophyll-binding protein degradation during senescence. Trends Plant Sci 14:155–162

Hu Z, Deng L, Chen X, Wang P, Chen G (2010) Co-suppression of the EIN2-homology gene LeEIN2 inhibits fruit ripening and reduces ethylene sensitivity in tomato. Russ J Plant Physiol 57:554–559

Isaacson T, Ronen G, Zamir D, Hirschberg J (2002) Cloning of *tangerine* from tomato reveals a carotenoid isomerase essential for the production of β-carotene and xanthophylls in plants. Plant Cell 14:333–342

Ju CL, Yoon GM, Shemansky JM, Lin DY, Ying ZI, Chang JH, Garrett WM, Kessenbrock M, Groth G, Tucker ML, Cooper B, Kieber JJ, Chang C (2012) CTR1 phosphorylates the central regulator EIN2 to control ethylene hormone signaling from the ER membrane to the nucleus in Arabidopsis. Proc Natl Acad Sci USA 109:19486–19491

Jun S-H, Han M-J, Lee S, Seo YS, Kim WT, An G (2004) OsEIN2 is a positive component in ethylene signaling in rice. Plant Cell Physiol 45:281–289

Kachanovsky DE, Filler S, Isaacson T, Hirschberg J (2012) Epistasis in tomato color mutations involves regulation of *phytoene synthase 1* expression by *cis*-carotenoid. Proc Natl Acad Sci USA 109:19021–19026

Kang B, Gu Q, Tian P, Xiao L, Cao H, Yang W (2014) A chimeric transcript containing *Psy1* and a potential mRNA is associated with *yellow flesh* color in tomato accession PI 114490. Planta 240:1011–1021

Karlova R, Chapman N, David K, Angenent GC, Seymour GB, de Maagd RA (2014) Transcriptional control of fleshy fruit development and ripening. J Exp Bot 65:4527–4541

Kilambi HV, Kumar R, Sharma R, Sreelakshmi Y (2013) Chromoplast-specific carotenoid-associated protein appears to be important for enhanced accumulation of carotenoid in *hp1* tomato fruits. Plant Physiol 161:2085–2101

Klee HJ, Giovannoni JJ (2011) Genetics and control of tomato fruit ripening and quality attributes. Annu Rev Genet 45:41–59

Lanahan MB, Yen HC, Giovannoni JJ, Klee HJ (1994) The *never ripe* mutation blocks ethylene perception in tomato. Plant Cell 6:521–530

Levin I, Frankel P, Gilboa N, Tanny S, Lalazar A (2003) The tomato *dark green* mutation is a novel allele of the tomato homolog of the *DEETIOLATED1* gene. Theor Appl Genet 106:454–460

Li W, Chetelat RT (2010) A pollen factor linking inter- and intraspecific pollen rejection in tomato. Science 330:1827–1830

Lieberman M, Segev O, Gilboa N, Lalazar A, Levin I (2004) The tomato homolog of the gene encoding UV-damaged DNA binding protein 1 (DDB1) underlined as the gene that causes the *high pigment-1* mutant phenotype. Theor Appl Genet 108:1574–1581

Lin T, Zhu GT, Zhang JH, Xu XY, Yu QH, Zheng Z, Zhang ZH, Lun YY, Li S, Wang XX, Huang ZJ, Li JM, Zhang CZ, Wang TT, Zhang YY, Wang AX, Zhang YC, Lin K, Li CY, Xiong GH, Xue YB, Mazzucato A, Causse M, Fei ZJ, Giovannoni JJ, Chetelat RT, Zamir D, Städler T, Li JF, Ye ZB, Du YC, Huang SW (2014) Genomic analyses provide insights into the history of tomato breeding. Nat Genet 46:1220–1226

Ma N, Feng H, Meng X, Li D, Yang D, Wu C, Meng Q (2014) Overexpression of tomato *SlNAC1* transcription factor alters fruit pigmentation and softening. BMC Plant Biol 14:351

Manning K, Tör M, Poole M, Hong Y, Thompson AJ, King GJ, Giovannoni JJ, Seymour GB (2006) A naturally occurring epigenetic mutation in a gene encoding an SBP-box transcription factor inhibits tomato fruit ripening. Nat Genet 38:948–952

Matas AJ, Yeats TH, Buda GJ, Zheng Y, Chatterjee S, Tohge T, Ponnala L, Adato A, Aharoni A, Stark R, Fernie AR, Fei Z, Giovannoni JJ, Rose JK (2011) Tissue- and cell-type specific transcriptome profiling of expanding tomato fruit provides insights into metabolic and regulatory specialization and cuticle formation. Plant Cell 23:3893–3910

Mathews H, Clendennen SK, Caldwell CG, Liu XL, Connors K, Matheis N, Schuster DK, Menasco DJ, Wagoner W, Lightner J, Wagner DR (2003) Activation tagging in tomato identifies a transcriptional regulator of anthocyanin biosynthesis, modification, and transport. Plant Cell 15:1689–1703

Menda N, Semel Y, Peled D, Eshed Y, Zamir D (2004) In silico screening of a saturated mutation library of tomato. Plant J 38:861–872

Moyle LC (2008) Ecological and evolutionary genomics in the wild tomatoes (*Solanum* Sect. *Lycopersicon*). Evolution 62:2995–3013

Muir SR, Collins GJ, Robinson S, Hughes S, Bovy A, De Vos CHR, van Tunen AJ, Verhoeyen ME (2001) Overexpression of petunia chalcone isomerase in tomato results in fruit containing increased levels of flavonols. Nat Biotechnol 19:470–474

Mustilli AC, Fenzi F, Ciliento R, Alfano F, Bowler C (1999) Phenotype of the tomato *high pigment-2* mutant is caused by a mutation in the tomato homolog of *DEETIOLATED1*. Plant Cell 11:145–158

Neto CC (2007) Cranberry and blueberry: evidence for protective effects against cancer and vascular diseases. Mol Nutr Food Res 51:652–664

Oeller PW, Lu MW, Taylor LP, Pike DA, Theologis A (1991) Reversible inhibition of tomato fruit senescence by antisense RNA. Science 254:437–439

Osorio S, Alba R, Damasceno CM, Lopez-Casado G, Lohse M, Zanor MI, Tohge T, Usadel B, Rose JK, Fei Z, Giovannoni JJ, Fernie AR (2011) Systems biology of tomato fruit development: combined transcript, protein and metabolite analysis of tomato transcription factor (*nor, rin*) and ethylene receptor (*Nr*) mutants reveals novel regulatory interactions. Plant Physiol 157:405–425

Picton S, Barton SL, Bouzayen M, Hamilton AJ, Grierson D (1993) Altered fruit ripening and leaf senescence in tomatoes expressing an antisense ethylene-forming enzyme transgene. Plant J 3:469–481

Qiao H, Shen ZX, Huang SSC, Schmitz RJ, Urich MA, Briggs SP, Ecker JR (2012) Processing and subcellular trafficking of ER-Tethered EIN2 control response to ethylene Gas. Science 338:390–393

Riccioni G (2009) Carotenoid and cardiovascular disease. Curre Atheroscler Rep 11:434–439

Ronen G, Cohen M, Zamir D, Hirschberg J (1999) Regulation of carotenoid biosynthesis during tomato fruit development: expression of the gene for lycopene epsilon-cyclase is down-regulated during ripening and is elevated in the mutant *Delta*. Plant J 17:341–351

Ronen G, Carmel-Goren L, Zamir D, Hirschberg J (2000) An alternative pathway to β-carotene formation in plant chromoplasts discovered by map-based cloning of *Beta* and *old-gold* color mutations in tomato. Proc Natl Acad Sci USA 97:11102–11107

Rosati C, Diretto G, Giuliano G (2010) Biosynthesis and engineering of carotenoid and apocarotenoid in plants: state of the art and future prospects. Biotechnol Genet Eng Rev 26:139–162

Schijlen EG, de Vos CR, Martens S, Jonker HH, Rosin FM, Molthoff JW, Tikunov YM, Angenent GC, van Tunen AJ, Bovy AG (2007) RNA interference silencing of chalcone synthase, the first step in the flavonoid biosynthesis pathway, leads to parthenocarpic tomato fruits. Plant Physiol 144:1520–1530

Schweiggert RM, Steingass CB, Heller A, Esquivel P, Carle R (2011) Characterization of chromoplasts and carotenoid of red-and yellow-fleshed papaya (*Carica papaya L.*). Planta 234:1031–1044

Seeram NP, Adams LS, Hardy ML, Heber D (2004) Total cranberry extract versus its phytochemical constituents: antiproliferative and synergistic effects against human tumor cell lines. J Agric Food Chem 52:2512–2517

Shibuya K, Barry KG, Ciardi JA, Loucas HM, Underwood BA, Nourizadeh S, Ecker JR, Klee HJ, Clark DG (2004) The central role of PhEIN2 in ethylene responses throughout plant development in petunia. Plant Physiol 136:2900–2912

Spooner DM, Peralta IE, Knapp S (2005) Comparison of AFLPs with other markers for phylogenetic inference in wild tomatoes (*Solanum* L. section *Lycopersicon* (Mill.) Wettst.). Taxon 54:43–61

Tanksley SD (2004) The genetic, developmental, and molecular bases of fruit size and shape variation in tomato. Plant Cell 16:181–189

Tomato Genome Consortium (2012) The tomato genome sequence provides insights into fleshy fruit evolution. Nature 485:635–641

Vrebalov J, Ruezinsky D, Padmanabhan V, White R, Medrano D, Drake R, Schuch W, Giovannoni J (2002) A MADS-box gene necessary for fruit ripening at the tomato *ripening-inhibitor* (*rin*) locus. Science 296:343–346

Wang J, Wen C-K (2015) Cryptic Role of the ETHYLENE INSENSITIVE2 nuclear localization signal in ethylene signaling. Mol Plant 8:1129–1130

Wang J, Chen G, Hu Z, Chen X (2007) Cloning and characterization of the EIN2-homology gene LeEIN2 from tomato. Mitochondrial DNA 18:33–38

Wang L, Li B, Pan MX, Mo XF, Chen YM, Zhang CX (2014) Specific carotenoid intake is inversely associated with the risk of breast cancer among Chinese women. Br J Nutr 111:1686–1695

Wen X, Zhang CL, Ji YS, Zhao Q, He WR, An FY, Jiang LW, Guo HW (2012) Activation of ethylene signaling is mediated by nuclear translocation of the cleaved EIN2 carboxyl terminus. Cell Res 22:1613–1616

Wilkinson JQ, Lanahan MB, Yen H-C, Giovannoni JJ, Klee HJ (1995) An ethylene-inducible component of signal transduction encoded by *Never-ripe*. Science 270:1807–1809

Yeats TH, Howe KJ, Matas AJ, Buda GJ, Thannhauser TW (2010) Mining the surface proteome of tomato (*Solanum lycopersicum*) fruit for proteins associated with cuticle biogenesis. J Exp Bot 61:3759–3771

Yuan D, Chen J, Shen H, Yang W (2008) Genetics of flesh color and nucleotide sequence analysis of phytoene synthase gene 1 in a yellow-fruited tomato accession PI114490. Sci Hortic 118:20–24

Zhu HL, Zhu BZ, Shao Y, Wang XG, Lin XJ, Xie YH, Li YC, Gao HY, Luo YB (2006) Tomato fruit development and ripening are altered by the silencing of *LeEIN2* gene. J Integr Plant Biol 48:1478–1485

Zhu M, Chen G, Zhou S, Tu Y, Wang Y, Dong T, Hu Z (2014) A new tomato NAC (NAM/ATAF1/2/CUC2) transcription factor, SlNAC4, functions as a positive regulator of fruit Ripening and carotenoid accumulation. Plant Cell Physiol 55:119–135